Supporting Information: Resonance Fluorescence of GaAs Quantum Dots with Near-Unity Photon Indistinguishability

Eva Schöll,[†,‖] Lukas Hanschke,[‡,‖] Lucas Schweickert,[†,‖] Katharina D. Zeuner,[†] Marcus Reindl,[¶] Saimon Filipe Covre da Silva,[¶] Thomas Lettner,[†] Rinaldo Trotta,[§] Jonathan J. Finley,[‡] Kai Müller,[‡] Armando Rastelli,[¶] Val Zwiller,[†] and Klaus D. Jöns[*,†]

†*Department of Applied Physics, Royal Institute of Technology, Albanova University Centre, Roslagstullsbacken 21, 106 91 Stockholm, Sweden*

‡*Walter Schottky Institut and Physik Department, Technische Universität München, 85748, Garching, Germany*

¶*Institute of Semiconductor and Solid State Physics, Johannes Kepler University Linz, 4040, Austria*

§*Dipartimento di Fisica, Sapienza Università di Roma, Piazzale A. Moro 1, I-00185 Roma, Italy*

‖*E. Schöll, L. Hanschke, and L. Schweickert contributed equally to this work.*

E-mail: klausj@kth.se

Rabi oscillation

Our power dependent resonance fluorescence measurements show clear Rabi oscillations. We fit the data using the following equation[1]:

$$\rho_{ee}(t) = \frac{1}{2(1+2\chi^2)} \left(1 - \left(\cos(\Omega' t) + \frac{3\chi}{\sqrt{4-\chi^2}} \sin(\Omega' t) \right) \mathrm{e}^{-\frac{3\Gamma_1 t}{2}} \right), \tag{1}$$

where $\chi = \Gamma_1/\Omega_0$, $\Omega' = \sqrt{\Omega_0^2 - \Gamma_1^2/4}$, Ω_0 is the Rabi frequency and Γ_1 is the decay rate of the spontaneous emission. The Rabi frequency, given by $\Omega_0 = |-eE_0\mu_{12}/\hbar|$, with the electrical field E_0 and the dipole matrix element μ_{12}, is proportional to the excitation power since $\Omega_0 \propto E_0 \propto \sqrt{P}$. Therefore, the population under pulsed excitation can be expressed as a function of the pulse area

$$\Theta = \left| \frac{\mu_{12}}{\hbar} \int_{-\infty}^{\infty} E_0(t) dt \right| \tag{2}$$

with the excitation pulse envelope $\int_{-\infty}^{\infty} E_0(t) dt$. Since we only extract the population under π–pulse excitation, absolute values for the excitation power density are not needed.

Time-correlated single-photon counting fit function including convolution with internal response function

We recorded the internal response function of our full setup by time-correlated photon counting of a short laser pulse resonant to the quantum dot transition, attenuated to count rates similar to the quantum dot, and its electrical trigger signal. The internal response function is used for a convolution with our fitting function:

$$y_0 + \Theta(t - t_0) \times A_1 e^{\frac{-(t-t_0)}{\tau_{\mathrm{main}}}} \times A_2 \sin^2((t - t_1)/f) + \Theta(t - t_0) \times A_3 e^{\frac{-(t-t_0)}{\tau_{\mathrm{slow}}}}$$

Here, $\Theta(t - t_0)$ is the Heaviside step function, which is multiplied with our main decay and an additional slow decay. t_0 and t_1 act as offsets in time, τ_{main} and τ_{slow} are decay times and f defines the frequency of the modulation. The main decay corresponds to the excited state life time and is modulated by a sine squared for fitting the exciton time–correlated

single-photon counting data. We attribute the second slow decay with a decay time constant of $\tau_{\text{slow}} = (550 \pm 20)$ ps to spin flip–flop processes which give rise to an on–and–off blinking of the exciton transition. This second decay, with an amplitude 1000 times weaker than the main decay of the exciton, is not present for the trion and biexciton transitions (not shown), which makes it very likely that it indeed stems from spin flip–flop processes. We use the same fitting function, without the second slow decay and without the modulation to fit our trion time–correlated single-photon counting data.

Polarization resolved photoluminescence spectroscopy

To confirm the fine structure splitting of the exciton state, which we extracted from the oscillation in the time–correlated single-photon counting measurement, we recorded additional polarization resolved photoluminescence spectra under non–resonant excitation. For this we replaced the quarter- with a half waveplate before the polarizing beam splitter and recorded the quantum dot spectrum for different linear polarization angles and fitted the exciton transition with a Gaussian function. The corresponding measurement is depicted in Fig. S1 where we plot the exciton emission energy as a function of half waveplate angles. The data is

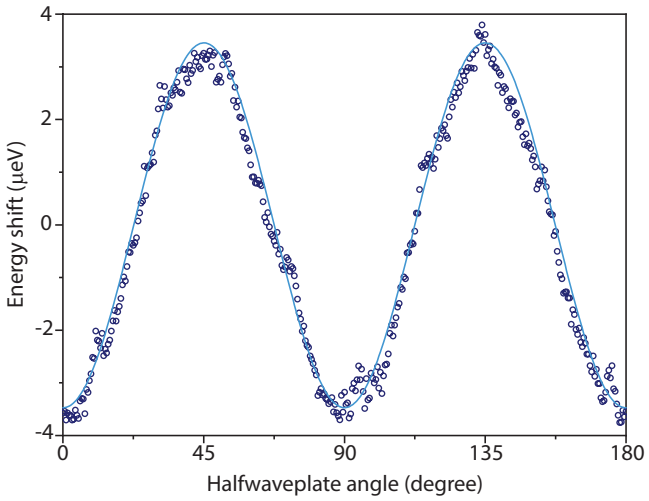

Figure S1: Center energy of exciton emission line fitted with a Gaussian peak plotted over half waveplate angle showing a fine structure splitting of $\Delta E_{\text{FSS}} = (7.0 \pm 0.5)$ µeV.

fitted with a sine squared function and the fine structure splitting $\Delta E_{\mathrm{FSS}} = (7.0 \pm 0.5)\,\mu\mathrm{eV}$ is given by the amplitude. Both measurements, the time–correlated single–photon counting in the main text and the polarization resolved photoluminescence shown here, agree well within the experimental error. Due to our high time resolution of 30 ps in the correlation measurements our statistical error is very small. Investigating the precession of the exciton in the time domain allows to measure the fine structure splitting with extremely high accuracy [2].

Analysis of two–photon interference measurements

We would like to point out that the quality of a fit to two-photon interference measurement data benefits strongly from high time resolution. In particular, it is crucial to be able to resolve possible quantum beats [3] and the dip (volcano shape) at time delay zero [4] in the measurement, otherwise the visibility will be overestimated when fitting the data. In Fig. S2 a), we show the raw data of the two–photon interference measurement of QD4, demonstrating that we can resolve quantum beats. Fig. S2 b) is a zoom in of the raw data around zero time delay, which shows the volcano shape resolved by our measurement. The reason for the above–mentioned overestimation is that the central peak will look like a single broader peak if the dip is not resolved. The error occurs when the data is fitted: The decay of all the quintuplet peaks are defined by the lifetime of the systems which is usually a shared fitting parameter of the quintuplet peaks.

Independently of the peak function used (ideally one should use the same fitting function as used for time-correlated single-photon counting, i.e. in the ideal case an exponential decay) the central peak width will be underestimated thanks to the larger statistics in the side peaks and the low maximum correlation events at time delay zero. To prove our point we artificially reduce our time resolution by binning the correlation data to time bins of 256 ps. The binned data is plotted in Fig. S2 c) to f). In all cases, the central peak of the quintuplet in the binned data does not show a sign of quantum beats and is not volcano

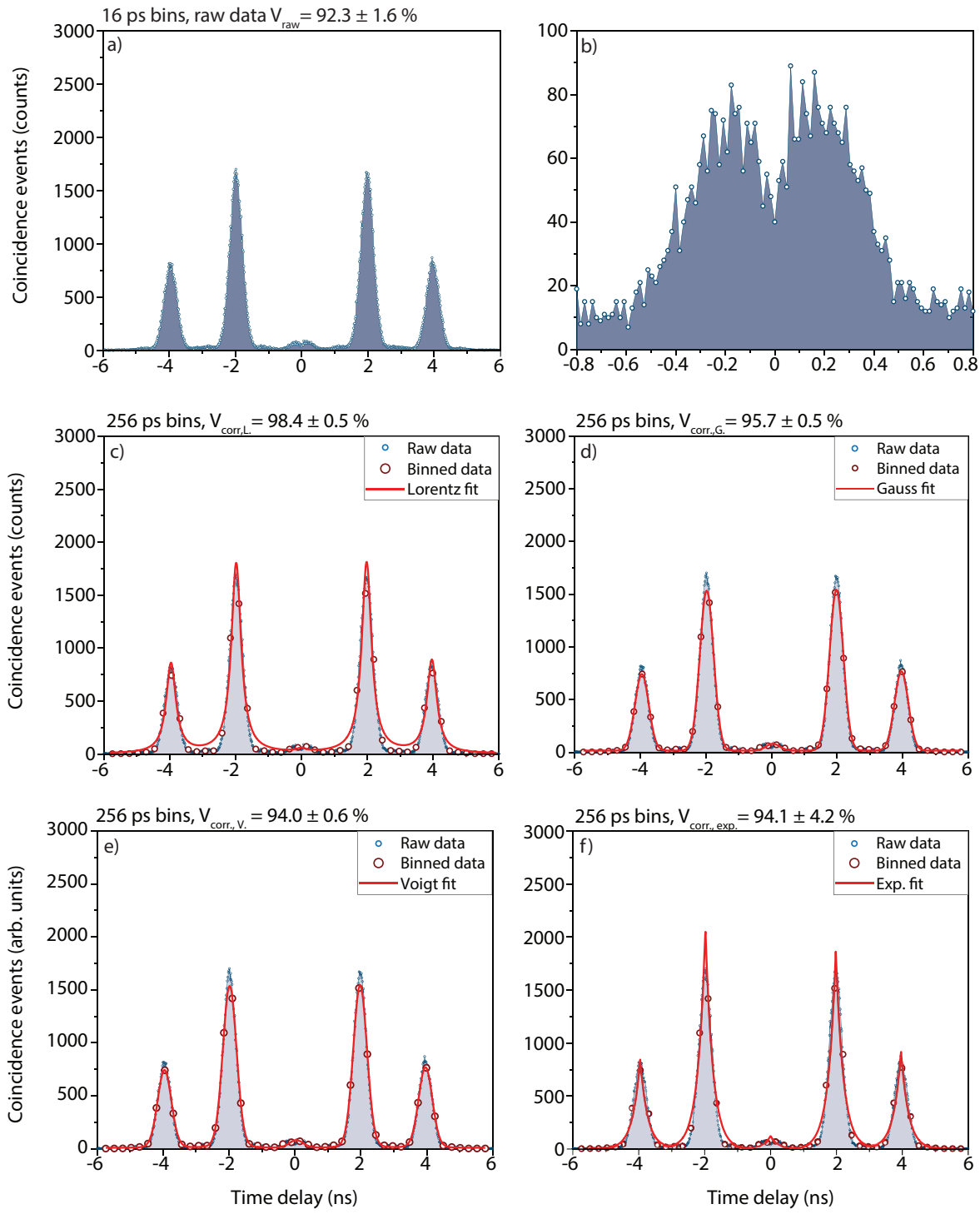

Figure S2: a) Raw data of the two–photon interference measurement under s–shell resonant excitation in time bins of 16 ps. b) Zoom in around zero time delay resolving the volcano shape due to high time resolution. c)-f) Data binned into 256 ps bins (red dots) and fitted with a series of five c) Lorentzian peaks, d) Gaussian fits, e) Voigt fits, and f) exponential decays (red lines). Original raw data is shown in light blue.

shaped, due to the too low time resolution. For a comparison we now fit the quintuplet with commonly used fit functions, i.e., Lorentzian functions (Fig. S2 c)), Gaussians (Fig. S2 d)), Voigts (Fig. S2 e)) and exponential decays (Fig. S2 f)) and extract a two-photon interference visibility of $V_{\mathrm{raw}} = 1 - \frac{2\times A_2}{A_1+A_3}$ from the fitted peak areas. The resulting visibilities, as well as the corrected visibilites are summarized in Table S1. This demonstrates that the visibility extracted from the binned data with reduced time resolution, independently of used fit function, is always overestimating the visibility compared to the raw data.

Table S1: Overview of Hong–Ou–Mandel visibilities for the same data with bins summed up (raw) and fitted with different functions corrected and uncorrected with the maximally achievable visibility in our setup. Results for three different quantum dots are shown.

		V_{raw} (%)	V_{Lorentz} (%)	V_{Gauss} (%)	V_{Voigt} (%)	$V_{\mathrm{Exponential}}$ (%)
QD1	uncorrected	$94.9^{+5.1}_{-6.4}$	97.8 ± 2.2	98.2 ± 1.8	96.5 ± 0.9	96.0 ± 2.2
	corrected	$97.3^{+2.7}_{-6.7}$	100.3 ± 2.2	100.7 ± 1.8	99.0 ± 0.9	$98.5^{+1.5}_{-2.2}$
QD2	uncorrected	92.6 ± 5.1	94.3 ± 4.7	94.5 ± 0.6	94.3 ± 0.6	94.7 ± 3.5
	corrected	$95.0^{+5.0}_{-5.3}$	$96.7^{+3.3}_{-4.8}$	96.9 ± 0.6	96.7 ± 0.6	$97.1^{+2.9}_{-3.5}$
QD4	uncorrected	92.3 ± 1.6	98.4 ± 0.5	95.7 ± 0.5	94.0 ± 0.6	94.1 ± 4.2
	corrected	94.7 ± 1.7	100.9 ± 0.5	98.2 ± 0.5	96.4 ± 0.6	$96.2^{+3.8}_{-4.3}$

This overestimation is more severe if the peaks overlap due to a too short time separation of the double excitation or due to a too long life time of the investigated quantum emitter transition. Due to the overlap simply adding all coincidences in a given time window is rarely used. However, in our opinion summing up in a carefully determined time window is the only reliable method to not overestimate the photon indistiguishability due to a fitting error.

This time window is determined as follows: Since neighboring peaks are slightly overlapping, the time delays, for which the overlapping areas are the same, have to be determined. Therefore, all peaks in the quintuplet are fitted with an exponential decay. The decay time is fixed in the fit and given by the lifetime of the transition which is extracted from a separate measurement using the fitting method explained above. Figure S3 a) shows a schematic histogram with a lifetime of 300 ps. The lifetime is chosen to be slightly higher compared to the typically measured lifetimes in order to make the overlap more visible. Figure S3 b) shows

the overlap of two neighboring peaks in more detail. The intersections of two neighboring fits mark the wanted time delay (orange line in Fig. S3 b)). Here the overlapping areas (dark red and blue) of two peaks are the same, as shown in the graph. We want to point out that this intersection is not in the middle of the two peaks (which would be at 3 ns in the shown case) and varies even more for intersections between the center peak and side peaks due to the much lower number of coincidence events in the center peak. This method leads to individual time windows for each transition, given by the lifetime and peak height. The determined time windows are summarized in Table S2 for all transitions.

Table S2: Overview of determined time windows for the calculation of Hong–Ou–Mandel visibilities and lifetime for comparison.

			Time window (ps)		
		Lifetime (ps)	Peak 1	Peak 2	Peak 3
QD1	Exciton	196	2352	1456	2368
	Trion	236	2400	1376	2384
QD2	Exciton	199	2336	1456	2336
	Trion	219	2320	1488	2336
QD3	Trion	228	2304	1520	2304
QD4	Exciton	199	2240	1648	2256

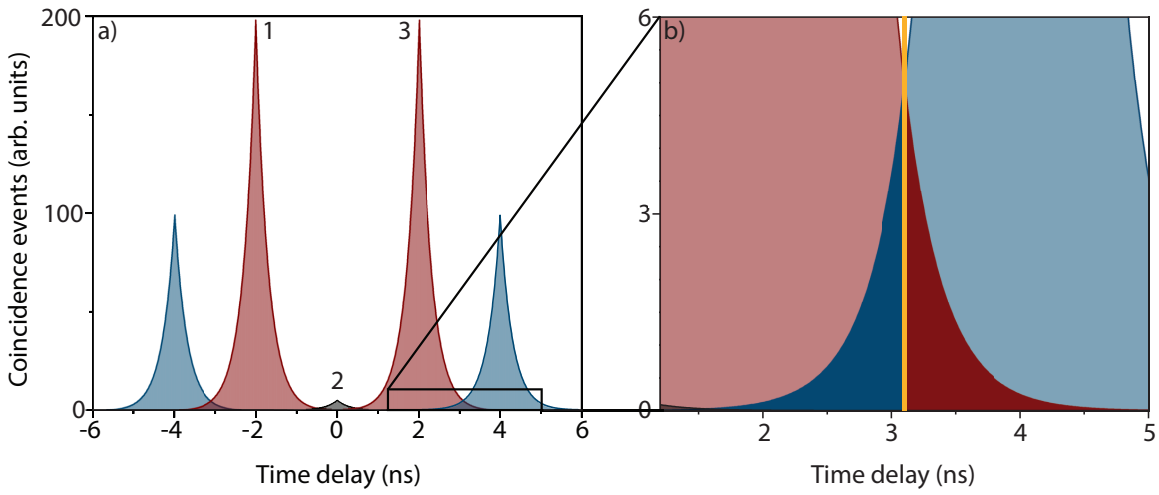

Figure S3: a) Schematic histogram with exponential decays and a lifetime of 300 ps. b) Zoom–in of the area marked with a black rectangle in a). The overlapping areas (dark blue and red) of the peaks are the same, when cutting at the time delay where the peaks intersect.

References

(1) Fox, M. *Quantum Optics: An Introduction*; OUP Oxford, 2006.

(2) Fognini, A.; Ahmadi, A.; Zeeshan, M.; Fokkens, J. T.; Gibson, S. J.; Sherlekar, N.; Daley, S. J.; Dalacu, D.; Poole, P. J.; Jöns, K. D.; Zwiller, V.; Reimer, M. E. *arXiv e-prints* **2017**, arXiv:1710.10815.

(3) Legero, T.; Wilk, T.; Hennrich, M.; Rempe, G.; Kuhn, A. *Phys. Rev. Lett.* **2004**, *93*, 070503.

(4) Kiraz, A.; Atatüre, M.; Imamoğlu, A. *Phys. Rev. A* **2004**, *69*, 032305.